Supporting Information

Systematic Analysis of Reaction Parameters Driving the Hydrothermal Growth of Layered VS_2

H. K. Shahzad[a], Zhengri Huang[a], Sasan Ghashghaie[a], Liu Han[a], G. Muhyodin[a], Mohsen Tamtaji[b], Hoi Lam Li[a], F. Chuan Chan[a], C. Y. Chung[a]

[a] *Department of Materials Science and Engineering, City University of Hong Kong, Kowloon Tong, Hong Kong SAR, China*

[b] *Department of Chemical and Biological Engineering, The Hong Kong University of Science and Technology, Clear Water Bay, Kowloon, Hong Kong, China*

Table S1. Reported hydrothermal growth parameters for VS_2 in literature

Product	Molar Ratio of NH_4VO_3: TAA	Solvent volume (mL)	$NH_3/NH_3.H_2O$ (mL)	Temp. (˚C)	Time (h)	Ref.
VS_2 NSs	1:7.5	[a)]DI water (30)	2	180	20	[1]
G-VS_2	1:10	DI water (30)	6	180	20	[2]
VS_2 NFs	1:5	DI water (15)	3	180	20	[3]
VS_2	1:7.5	DI water (60)	5	200	20	[4]
VS_2 NFs	1:4	DI water (45)	9	160	20	[5]
VS_2/GNS	1:5	DI water (30)	6	180	20	[6]
VS_2 NSs	1:5	DI water (15)	3	180	20	[7]
VS_2 NSs	1:7.5	DI water (30)	2	160	24	[8]
VS_2 NSs	1:7.5	DI water (30)	2	180	10	[9]
VS_2 NSs	1:10	DI water (40)	2	180	24	[10]
VS_2 NSs	1:7.5	DI water (30)	2	180	20	[11]
VS_2-GO	1:10	[b)]dist. water (30)	2	180	20	[12]
VS_2-MNSs	1:10	dist. water (30)	2	180	20	[13]
VS_2 Fs	1:5	DI water (15)	3	180	20	[14]
G-VS_2	1:10	DI water (30)	2	180	20	[15]
VS_2 NSs	1:70	DI water (30)	4	180	20	[16]

[a)]DI (de-ionized), [b)]dist. (distilled)

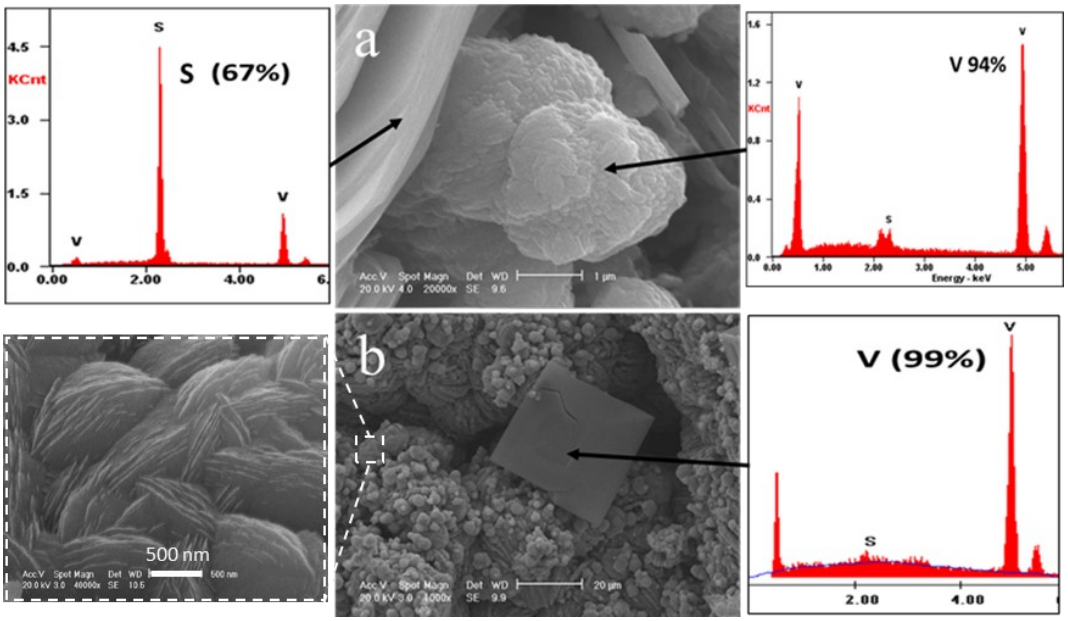

Figure S1. SEM images at different magnifications of the samples are shown in Row-1 (1: 2.5), and Row-2 (3:5) with selected EDX analysis

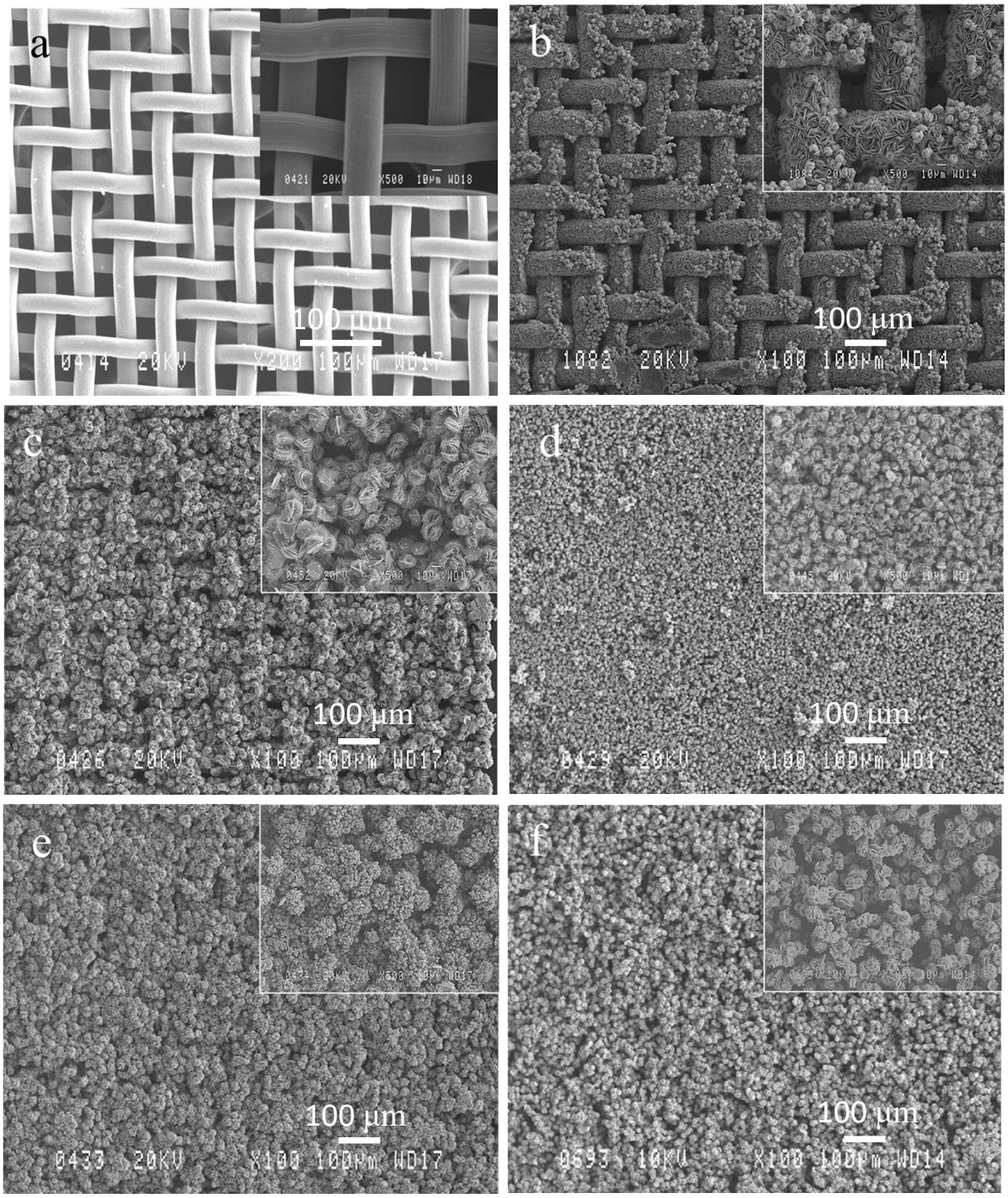

Figure S2. SEM micrographs of VS_2/SS prepared with different precursors' mass loadings (a) 0 mmol to 0 mmol (b) 2 mmol to 15 mmol (c) 3 mmol to 22.5 mmol (d) 4 mmol to 30 mmol (e) 5 mmol to 37.5 mmol (f) 6 mmol to 45 mmol

Figure S2 presents SEM micrographs illustrating the morphological changes of VS_2 nanosheets as precursor loading increases. At a 2x molar ratio (2 mmol: 15 mmol), the SS mesh was uniformly covered with laterally grown VS_2 nanoflakes, with small clusters of VS_2 microspheres (~10 µm in diameter) observed atop these flakes (Figure S2b).

At 3x loading (3 mmol: 22.5 mmol), the flower-like VS_2 nanosheets became more prominent, and their increased density enhanced surface coverage (Figure S2c). With further increases to 4x (4 mmol: 30 mmol), these structures merged to form a denser network, gradually filling the interwoven pores of the SS mesh (Figure S2d).

This trend is further corroborated by optical photographs taken under daylight conditions (Figure S3), where the increasing precursor loading visibly enhances VS_2 surface coverage, leading to the formation of a uniform, continuous film across the mesh. At even higher precursor loadings (5x = 5 mmol: 37.5 mmol and 6x = 6 mmol: 45 mmol), thicker porous VS_2 layers developed, with interconnected microspheres forming compact networks (Figure S2e-f). However, beyond 6x, excessive stacking led to multilayer formation, potentially compromising structural integrity due to material delamination or breakage during handling.

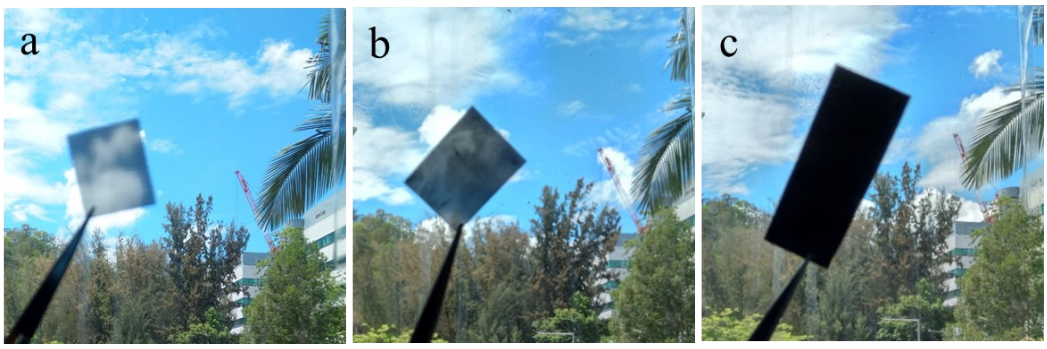

Figure S3. Optical photographs of SS/VS_2 prepared with three different mass loadings (a) 1 mmol to 7.5 mmol (b) 2 mmol to 15 mmol (c) 3 mmol to 22.5 mmol

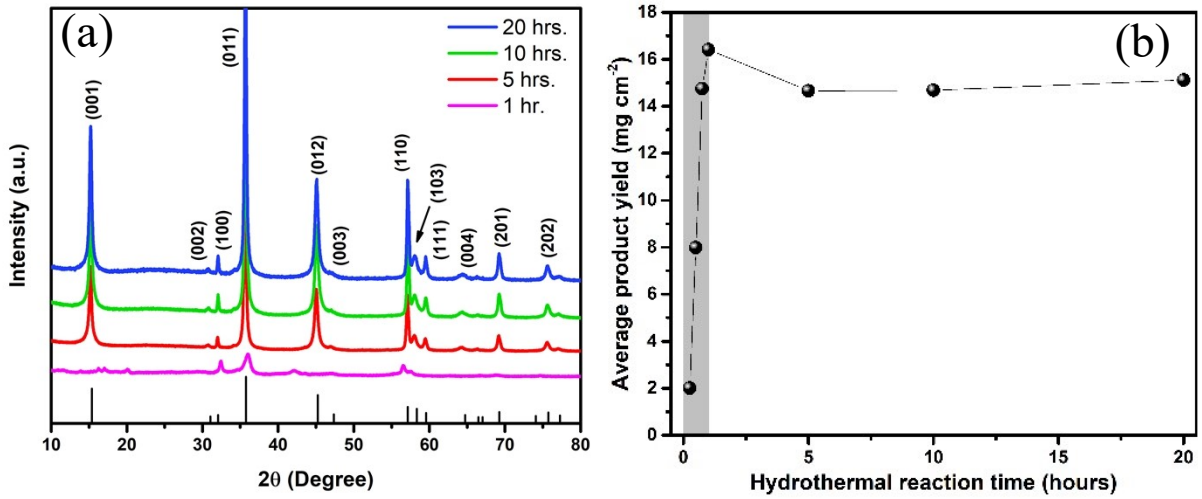

Figure S4. (a) XRD pattern of the SS/VS_2 synthesized at different reaction times (1, 5, 10, and 20 hours) (b) Average product yield obtained on the mesh after different batches of hydrothermal reaction times

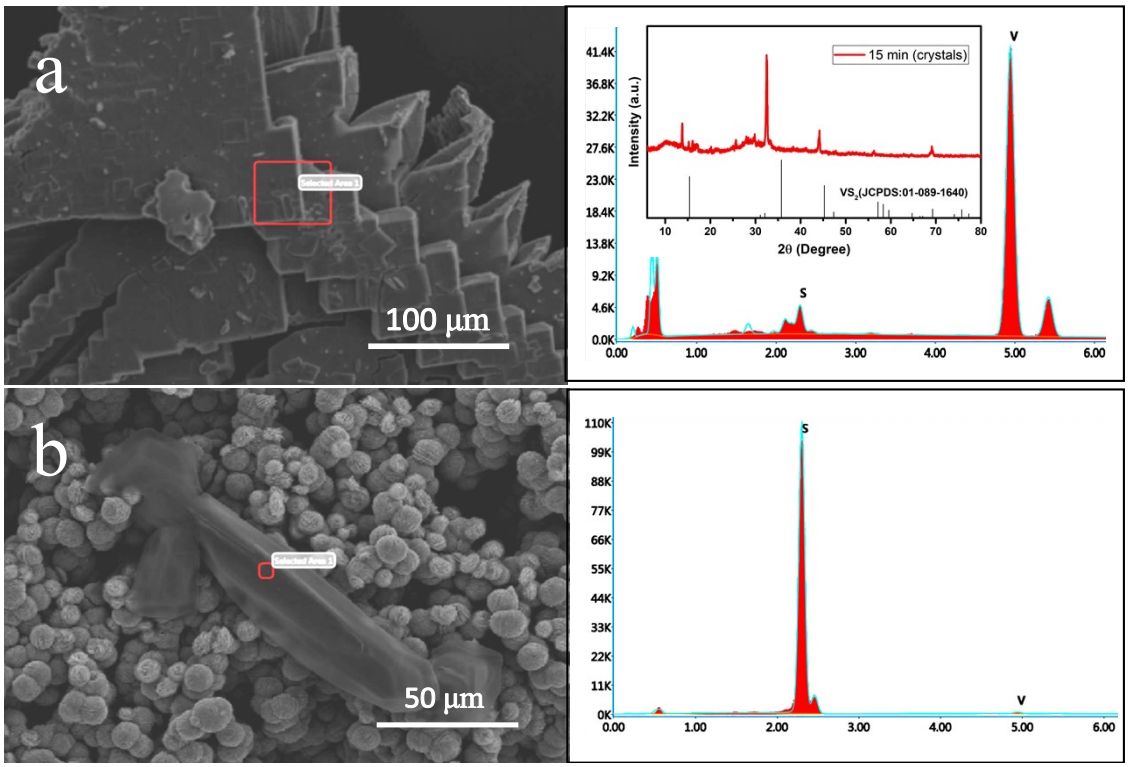

Figure S5. The EDX analysis of (a) massive dendritic crystal, (b) the translucent phase

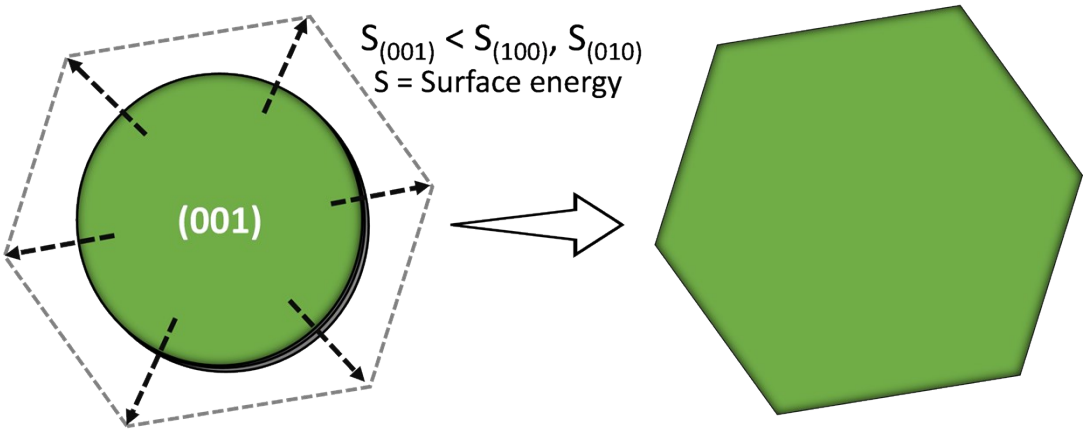

Figure S6. Schematic of anisotropic growth of VS_2 hexagonal crystal

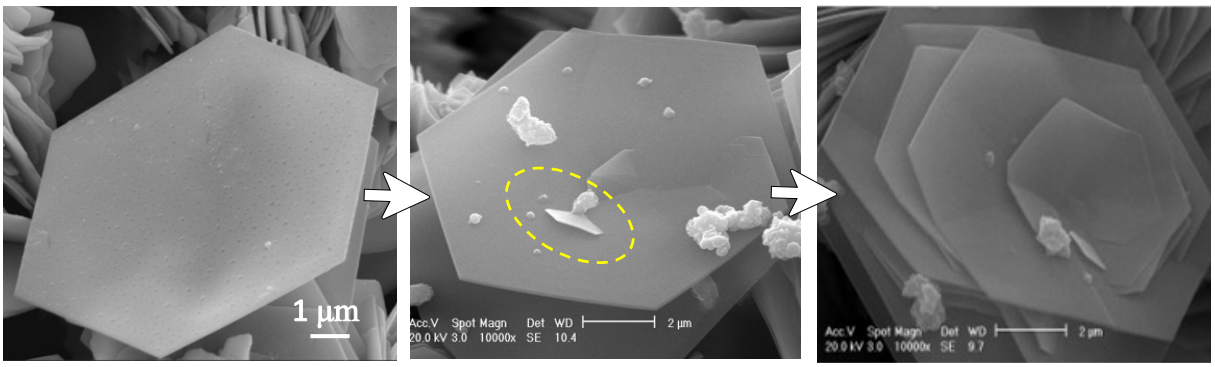

Figure S7. SEM images representing various growth stages of flower-likeVS_2 microsphere composed of hexagonal nanosheets

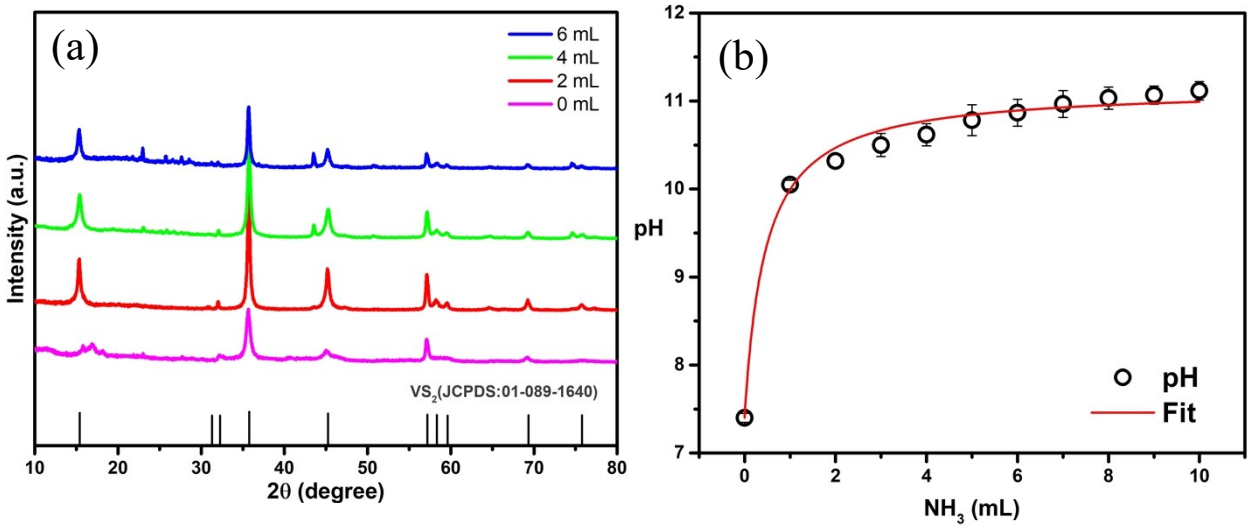

Figure S8. (a) XRD patterns of SS/VS_2 synthesized by adding 0 mL, 2 mL, 4 mL, and 6 mL of ammonia solution in the reaction vessel during hydrothermal reaction (b) Relationship of pH with the amount of ammonia in the solution

References

[1] He P, Yan M, Zhang G, Sun R, Chen L, An Q, et al. Layered VS_2 Nanosheet-Based Aqueous Zn Ion Battery Cathode. Adv Energy Mater 2017;7:1601920. https://doi.org/10.1002/AENM.201601920.

[2] Zhu X, Zhao W, Song Y, Li Q, Ding F, Sun J, et al. In Situ Assembly of 2D Conductive Vanadium Disulfide with Graphene as a High-Sulfur-Loading Host for Lithium–Sulfur Batteries. Adv Energy Mater 2018;8:1–9. https://doi.org/10.1002/aenm.201800201.

[3] Zhong M, Li Y, Xia Q, Meng X, Wu F, Li J. Ferromagnetism in VS_2 nanostructures: Nanoflowers versus ultrathin nanosheets. Mater Lett 2014;124:282–5. https://doi.org/10.1016/J.MATLET.2014.03.110.

[4] Mao M, Ji X, Hou S, Gao T, Wang F, Chen L, et al. Tuning Anionic Chemistry To Improve Kinetics of Mg Intercalation. Chemistry of Materials 2019;31:3183–91. https://doi.org/10.1021/ACS.CHEMMATER.8B05218.

[5] Chen X, Yu K, Shen Y, Feng Y, Zhu Z. Synergistic Effect of MoS_2 Nanosheets and VS_2 for the Hydrogen Evolution Reaction with Enhanced Humidity-Sensing Performance. ACS Appl Mater Interfaces 2017;9:42139–48. https://doi.org/10.1021/ACSAMI.7B14957.

[6] Fang W, Zhao H, Xie Y, Fang J, Xu J, Chen Z. Facile Hydrothermal Synthesis of VS_2 /Graphene Nanocomposites with Superior High-Rate Capability as Lithium-Ion Battery Cathodes 2015. https://doi.org/10.1021/acsami.5b03124.

[7] Masikhwa TM, Barzegar F, Dangbegnon JK, Bello A, Madito MJ, Momodu D, et al. Asymmetric supercapacitor based on VS_2 nanosheets and activated carbon materials. RSC Adv 2016;6:38990–9000. https://doi.org/10.1039/C5RA27155J.

[8] Yin BS, Zhang SW, Xiong T, Shi W, Ke K, Lee WSV, et al. Engineering sulphur vacancy in VS_2 as high performing zinc-ion batteries with high cyclic stability. New Journal of Chemistry 2020;44:15951–7. https://doi.org/10.1039/D0NJ02917C.

[9] Jiao T, Yang Q, Wu S, Wang Z, Chen D, Shen D, et al. Binder-free hierarchical VS_2 electrodes for high-performance aqueous Zn ion batteries towards commercial level mass loading. J Mater Chem A Mater 2019;7:16330–8. https://doi.org/10.1039/C9TA04798K.

[10] Zhang X, He Q, Xu X, Xiong T, Xiao Z, Meng J, et al. Insights into the Storage Mechanism of Layered VS_2 Cathode in Alkali Metal-Ion Batteries. Adv Energy Mater 2020;10:1904118. https://doi.org/10.1002/AENM.201904118.

[11] Haider WA, Tahir M, He L, Yang W, Minhas-khan A, Owusu KA, et al. Integration of VS_2 nanosheets into carbon for high energy density micro-supercapacitor. J Alloys Compd 2020;823:151769. https://doi.org/10.1016/J.JALLCOM.2019.151769.

[12] Sun R, Pei C, Sheng J, Wang D, Wu L, Liu S, et al. High-rate and long-life VS_2 cathodes for hybrid magnesium-based battery. Energy Storage Mater 2018;12:61–8. https://doi.org/10.1016/J.ENSM.2017.11.012.

[13] Sun R, Wei Q, Sheng J, Shi C, An Q, Liu S, et al. Novel layer-by-layer stacked VS_2 nanosheets with intercalation pseudocapacitance for high-rate sodium ion charge storage. Nano Energy 2017;35:396–404. https://doi.org/10.1016/J.NANOEN.2017.03.036.

[14] Liu J. Z. and Guo P. F. "VS_2 Nanosheets: A Potential Anode Materiral for Li-ion Batteriers." Journal of Inorganic Materials 2015;30,:1339-1344.

[15] Lu Wu, Ruimin Sun, Fangyu Xiong, Cunyuan Pei, Kang Han, Chen Peng, et al. A rechargeable aluminum-ion battery based on a VS_2 nanosheet cathode. Physical Chemistry Chemical Physics 2018;20:22563–8. https://doi.org/10.1039/C8CP04772C.

[16] Zhang L, Sun D, Wei Q, Ju H, Feng J, Zhu J, et al. Understanding the electrochemical reaction mechanism of VS_2 nanosheets in lithium-ion cells by multiple in situ and ex situ x-ray spectroscopy. J Phys D Appl Phys 2018;51:494001. https://doi.org/10.1088/1361-6463/AADDE7.